Electronic Supplementary Material to: A New Index Developed for Fast Diagnosis of Meteorological Roles in Ground-Level Ozone Variations

Weihua CHEN[1], Weiwen WANG[1], Shiguo JIA[2], Jingying MAO[1], Fenghua YAN[1], Lianming ZHENG[1], Yongkang WU[1], Xingteng ZHANG[1], Yutong DONG[1], Lingbin KONG[1], Buqing ZHONG[3], Ming CHANG[1], Min SHAO[1], and Xuemei WANG[1]

[1]*Guangdong-Hongkong-Macau Joint Laboratory of Collaborative Innovation for Environmental Quality, Institute for Environmental and Climate Research, Jinan University, Guangzhou* 510632, *China*

[2]*School of Atmospheric Sciences, Guangdong Province Key Laboratory for Climate Change and Natural Disaster Studies, Sun Yat-sen University, Guangzhou* 510275, *China*

[3]*Key Laboratory of Vegetation Restoration and Management of Degraded Ecosystems, South China Botanical Garden, Chinese Academy of Sciences, Guangzhou* 510650, *China*

ESM to: Chen, W. H., and Coauthors, 2021: A new index developed for fast diagnosis of meteorological roles in ground-level ozone variations. *Adv. Atmos. Sci.*, https://doi.org/10.1007/s00376-021-1257-x.

Table S1. Statistics for T_2 and WS during 2013–2019.

	T_2 (°C)						WS (m s^{-1})					
	OBS	SIM	MB	RMSE	*R*	IOA	OBS	SIM	MB	RMSE	*R*	IOA
BTH	12.72	12.89	0.17	1.3	0.99	1.00	1.75	3.50	1.75	1.80	0.74	0.25
FWP	14.43	15.09	0.66	1.32	0.99	1.00	2.19	3.34	1.15	1.20	0.34	0.27
YRD	16.60	16.61	0.01	0.66	1.00	1.00	2.18	4.22	2.05	2.07	0.62	0.14
SCB	14.50	16.26	1.76	2.33	0.98	0.98	1.65	2.80	1.14	1.21	0.31	0.20
PRD	22.93	23.11	0.18	0.86	0.99	0.99	2.10	4.69	2.60	2.66	0.39	0.15

Table S2. Fitting parameters for historical 90th percentile MDA8-O_3 and MSI in the key regions with 95% confidence bounds.

Region	Slope	Intercept	R^2
BTH	66.1 (58.8, 73.3)	69.3 (61.0, 77.7)	0.80**
FWP	49.6 (44.2, 55.0)	66.3 (59.2, 73.4)	0.80**
YRD	54.1 (47.2, 61.0)	81.5 (74.3, 88.8)	0.75**
SCB	42.6 (37.0, 48.3)	60.7 (52.6, 68.8)	0.73**
PRD	33.6 (23.7, 43.4)	98.4 (86.6, 110.2)	0.36**

**Significant at the 0.01 level

* The online version of this article can be found at: https://doi.org/10.1007/s00376-021-1257-x.

Table S3. Summary of the meteorological contribution to O_3 concentration.

Region	Period	Season	Method*	Contribution	Reference
Northern China	2003–2015	Annual	KZ	<0%	Ma et al., 2016
Northern China	2013–2017	Summer	CMAQ	>100%	Ding et al., 2019
Northern China	2004–2012	Winter	GEOS-Chem	>100%	Lou et al., 2015
Northern China	2004–2012	Spring	GEOS-Chem	80%	Lou et al., 2015
Northern China	2004–2012	Summer	GEOS-Chem	61%	Lou et al., 2015
Northern China	2004–2012	Autumn	GEOS-Chem	78%	Lou et al., 2015
BTH	2012–2017	Summer	GEOS-Chem	49%	Dang and Liao, 2019
BTH	2013–2019	Summer	MLR	42%	Li et al., 2020
BTH	2015–2019	Annual	KZ	32%	Mousavinezhad et al., 2021
Eastern China	2013–2018	Summer	MLR	43%	Han et al., 2020
Eastern China	2003–2015	Summer	GEOS-Chem	44%	Sun et al., 2019
YRD	2012–2017	Summer	GEOS-Chem	84%	Dang and Liao, 2019
YRD	2013–2019	Summer	MLR	43%	Li et al., 2020
YRD	2013–2017	Annual	KZ	<10%	Yu et al., 2019
YRD	2013–2017	Summer	CMAQ	>100%	Ding et al., 2019
Southern China	2013–2017	Summer	CMAQ	>100%	Ding et al., 2019
Southern China	2004–2012	Winter	GEOS-Chem	82%	Lou et al., 2015
Southern China	2004–2012	Spring	GEOS-Chem	67%	Lou et al., 2015
Southern China	2004–2012	Summer	GEOS-Chem	>100%	Lou et al., 2015
Southern China	2004–2012	Autumn	GEOS-Chem	92%	Lou et al., 2015
PRD	2013–2019	Summer	MLR	73%	Li et al., 2020
PRD	2007–2017	Annual	KZ	15%	Yang et al., 2019
PRD	2015–2019	Annual	KZ	83%	Mousavinezhad et al., 2021
SCB	2013–2019	Summer	MLR	<0%	Li et al., 2020
SCB	2004–2012	Winter	GEOS-Chem	58%	Lou et al., 2015
SCB	2004–2012	Spring	GEOS-Chem	45%	Lou et al., 2015
SCB	2004–2012	Summer	GEOS-Chem	47%	Lou et al., 2015
SCB	2004–2012	Autumn	GEOS-Chem	44%	Lou et al., 2015

*The methods include statistical methods, i.e., the Kolmogorov–Zurbenko (KZ) filter method and multiple linear regression (MLR), and chemical transport models (CTMs), i.e., the Community Multiscale Air Quality (CMAQ) and the Goddard Earth Observing System Chemistry Global Chemical Transport Model (GEOS-Chem).

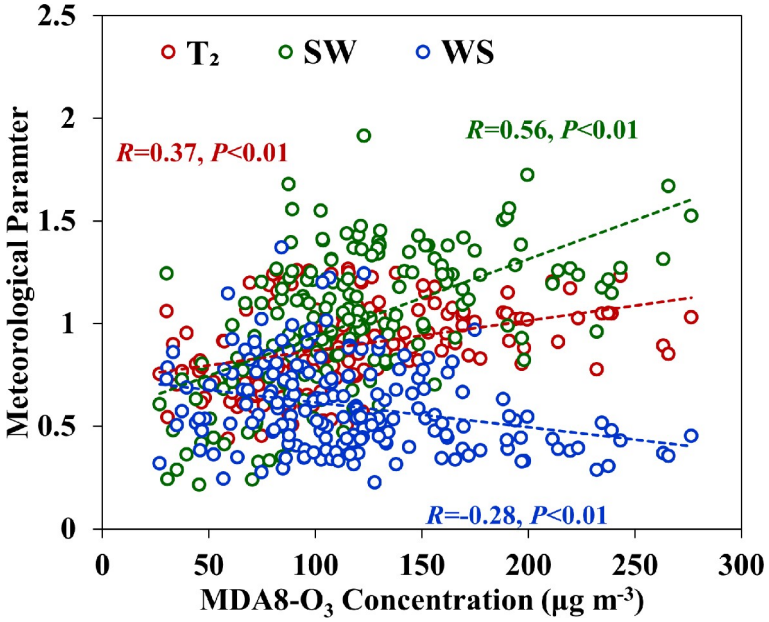

Fig. S1. Scatter plot of MDA8-O_3 concentration versus dimensionless meteorological parameters. The correlation coefficient is inserted.

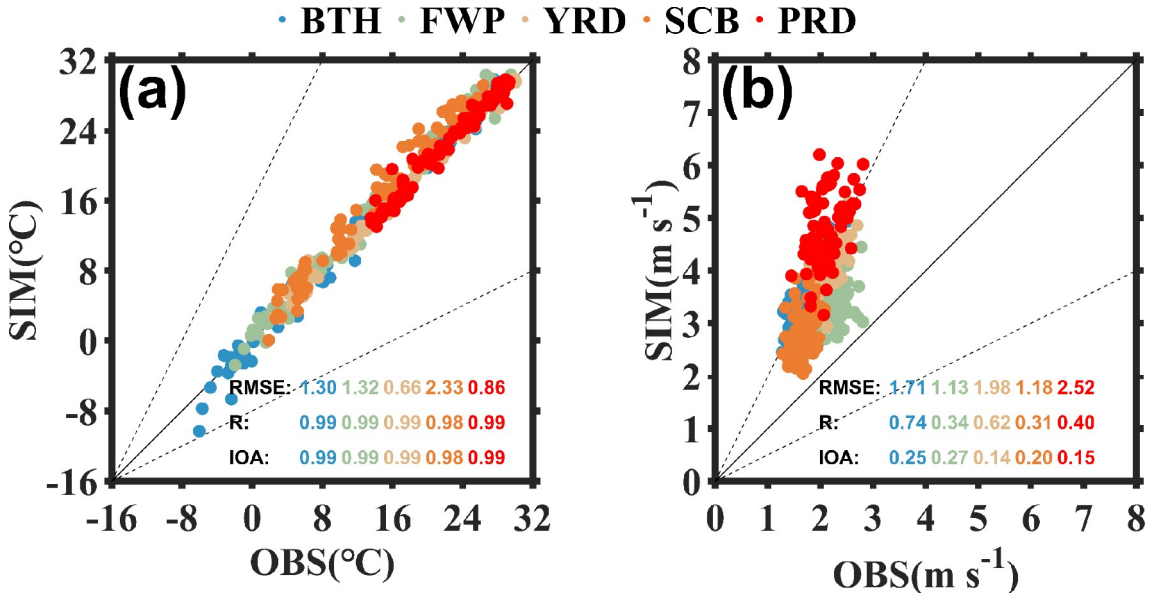

Fig. S2. Scatter plot of observed (OBS) versus simulated (SIM) (a) T_2 and (b) WS in the study regions over China from 2013 to 2019.

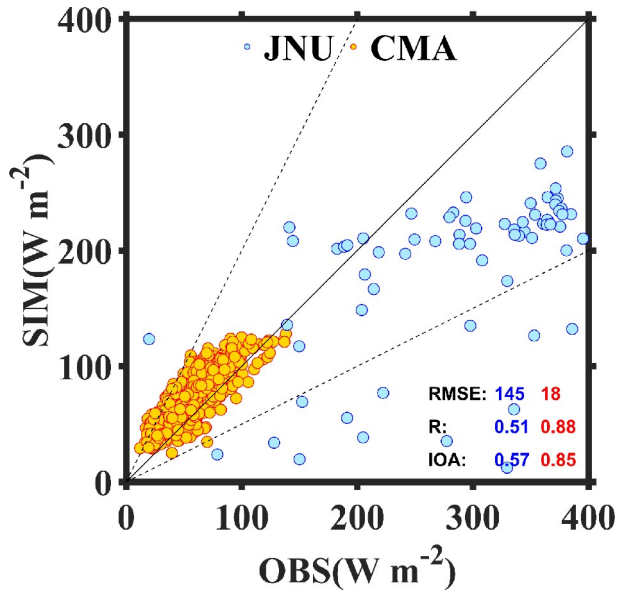

Fig. S3. Scatter plot of observed (OBS) versus simulated (SIM) SW. Blue dots represent daily solar radiation at JNU from 1 October 2019 to 31 December 2019; orange dots represent monthly solar radiation over China (CMA) from 2013 to 2019.

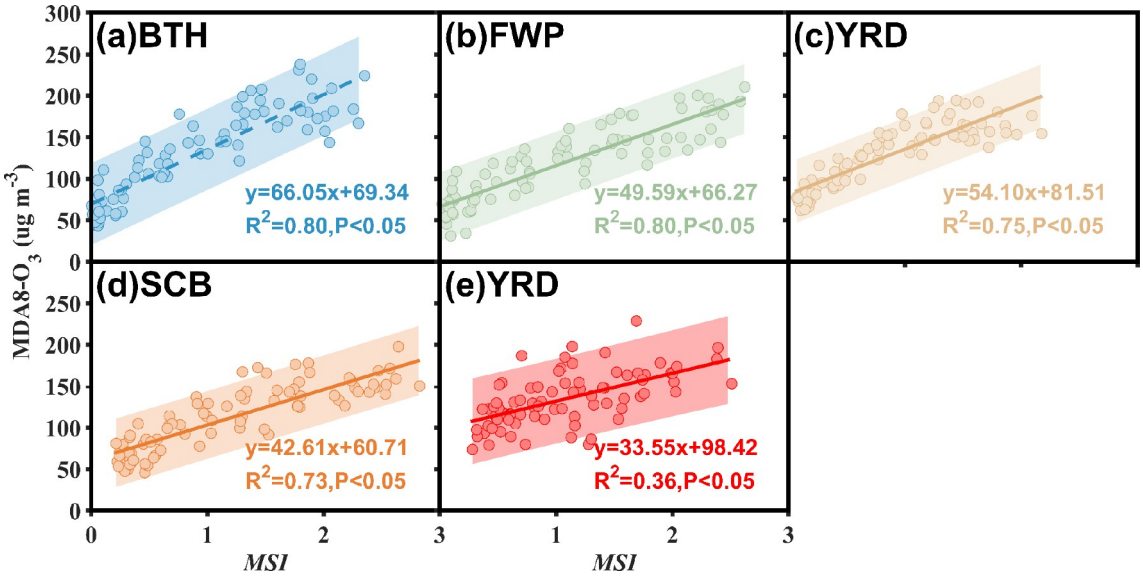

Fig. S4. Scatter plot of MSI versus observed MDA8-O_3 in the key regions over China during 2013–2019 (shaded areas are the 95% confidence interval).

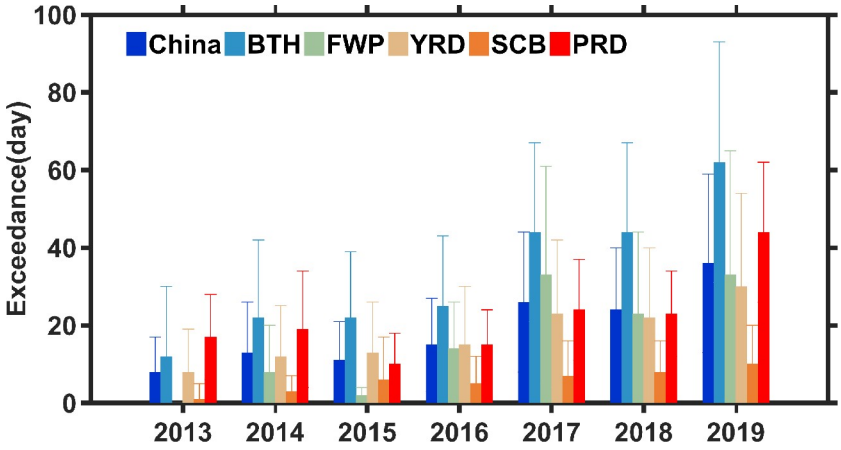

Fig. S5. Annual O_3 exceedance (days) in the study regions over China during 2013–2019.

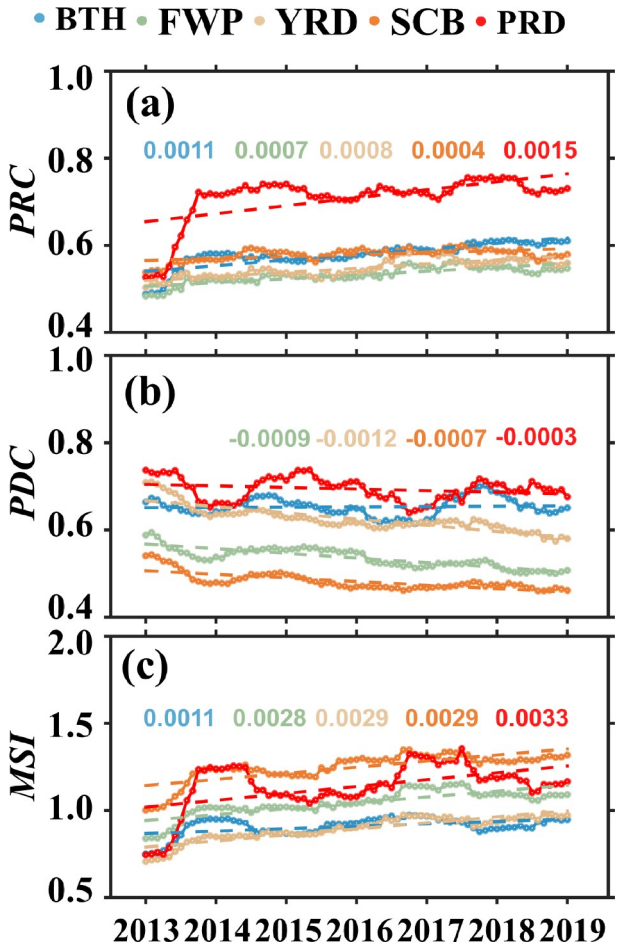

Fig. S6. Trends of the 12-month moving average (a) Photochemical Reaction Conditions (PRC), (b) Physical Dispersion Capacity (PDC), and (c) Meteorology Synthetic Index (MSI) in the study regions during 2013–2019. The slopes for the linear regression at the 95% confidence level are shown in each plot.

REFERENCES

Dang, R. J., and H. Liao, 2019: Radiative forcing and health impact of aerosols and ozone in China as the consequence of clean air actions over 2012–2017. *Geophys. Res. Lett.*, **46**, 12 511–12 519, https://doi.org/10.1029/2019GL084605.

Ding, D., J. Xing, S. X. Wang, X. Chang, and J. M. Hao, 2019: Impacts of emissions and meteorological changes on China's ozone pollution in the warm seasons of 2013 and 2017. *Frontiers of Environmental Science & Engineering*, **13**, 76, doi: https://doi.org/10.1007/s11783-019-1160-1.

Han, H., J. Liu, L. Shu, T. J. Wang, and H. L. Yuan, 2020: Local and synoptic meteorological influences on daily variability in summertime surface ozone in eastern China. *Atmospheric Chemistry and Physics*, **20**, 203–222, https://doi.org/10.5194/acp-20-203-2020.

Li, K., D. J. Jacob, L. Shen, X. Lu, I. De Smedt, and H. Liao, 2020: Increases in surface ozone pollution in China from 2013 to 2019: Anthropogenic and meteorological influences. *Atmospheric Chemistry and Physics*, **20**, 11 423–11 433, https://doi.org/10.5194/acp-20-11423-2020.

Lou, S. J., H. Liao, Y. Yang, and Q. Mu, 2015: Simulation of the interannual variations of tropospheric ozone over China: Roles of variations in meteorological parameters and anthropogenic emissions. *Atmos. Environ.*, **122**, 839–851, https://doi.org/10.1016/j.atmosenv.2015.08.081.

Ma, Z. Q., J. Xu, W. J. Quan, Z. Y. Zhang, W. L. Lin, and X. B. Xu, 2016: Significant increase of surface ozone at a rural site, north of eastern China. *Atmospheric Chemistry and Physics*, **16**, 3969–3977, https://doi.org/10.5194/acp-16-3969-2016.

Mousavinezhad, S., Y. Choi, A. Pouyaei, M. Ghahremanloo, and D. L. Nelson, 2021: A comprehensive investigation of surface ozone pollution in China, 2015–2019: Separating the contributions from meteorology and precursor emissions. *Atmospheric Research*, **257**, 105599, https://doi.org/10.1016/j.atmosres.2021.105599.

Sun, L., and Coauthors, 2019: Impacts of meteorology and emissions on summertime surface ozone increases over central eastern China between 2003 and 2015. *Atmospheric Chemistry and Physics*, **19**, 1455–1469, https://doi.org/10.5194/acp-19-1455-2019.

Yang, L. F., and Coauthors, 2019: Quantitative impacts of meteorology and precursor emission changes on the long-term trend of ambient ozone over the Pearl River Delta, China, and implications for ozone control strategy. *Atmospheric Chemistry and Physics*, **19**, 12 901–12 916, https://doi.org/10.5194/acp-19-12901-2019.

Yu, Y. J., Z. Wang, T. He, X. Y. Meng, S. Y. Xie, and H. X. Yu, 2019: Driving factors of the significant increase in surface ozone in the Yangtze River Delta, China, during 2013–2017. *Atmospheric Pollution Research*, **10**, 1357–1364, https://doi.org/10.1016/j.apr.2019.03.010.